The Journal of Allergy and Clinical Immunology
B cell-intrinsic requirement for STK4 in humoral immunity in mice and humans
--Manuscript Draft--

Abstract:	Humoral immune defects are described in 9 patients from 5 families with STK4 deficiency. A mouse model carrying the novel p.Y88del show that these defects are intrinsic to the B cells.

1 **Title page:**

2 **B cell-intrinsic requirement for STK4 in humoral immunity in mice and humans**

3 *Imogen Moran, PhD[1,2], Danielle T. Avery, BSc[1], Kathryn Payne, BSc[1], Helen Lenthall, MMSc[1], E.*

4 *Graham Davies, MD[3], Siobhan Burns, MD PhD[4,5], Winnie Ip, MD[3], Matÿfffedas M. Oleastro, MD[6],*

5 *Ismail Reisli, MD[7], Sukru Guner, MD[7], Sevgi Keles, MD[7], Luigi Notarangelo, MD[8], Elissa K.*

6 *Deenick, PhD[1,2], Christopher C. Goodnow, PhD[1,2], David Zahra, PhD[1], Robert Brink, PhD[1,2],*

7 *CIRCA[9], Melanie Wong, PhD[10,11]*, Stuart G. Tangye, PhD[1,2]*, Cindy S. Ma, PhD[1,2]*, Tri Giang*

8 *Phan, PhD[1,2]**

9 * Equal senior author

10 **From** [1]Immunology Division, Garvan Institute of Medical Research, Sydney, Australia; [2]St

11 Vincent's Clinical School, Faculty of Medicine, UNSW Sydney, Sydney, Australia; [3]Infection,

12 Immunity and Inflammation Theme, UCL Great Ormond Street Institute of Child Health, London,

13 United Kingdom; Department of Immunology, Great Ormond Street Hospital, London, United

14 Kingdom; [4]Department of Immunology, Royal Free London NHS Foundation Trust, London,

15 United Kingdom; [5]University College London, Institute of Immunity and Transplantation, London,

16 United Kingdom; [6]Immunology and Rheumatology Department, Hospital de Pediatría "Dr. Juan P.

17 Garrahan", Combate de los Pozos, 1881, Buenos Aires, Argentina; [7]Division of Pediatric

18 Immunology and Allergy, Meram Faculty of Medicine, Necmettin Erbakan University, Konya,

19 Turkey; [8]Laboratory of Clinical Immunology and Microbiology, National Institutes of Allergy and

20 Infectious Diseases, National Institutes of Health, Bethesda, Maryland, USA; [9]Clinical

21 Immunogenomics Research Consortium Australia; [10]Children's Hospital at Westmead, NSW,

22 Australia; [11]Faculty of Medicine, University of Sydney, Sydney, NSW, Australia.

23 **Correspondence:** Dr Tri Phan; Address: Garvan Institute of Medical Research, 384 Victoria St

24 Darlinghurst NSW Australia; Telephone: +61 2 92958414; Facsimile: +61 2 92958404; Email:

25 t.phan@garvan.org.au .

30 **Conflicts of interest:** The authors have no conflicts of interest to declare.

31 **Key finding:** Patients with STK4 deficiency have humoral immune defects due to intrinsic defects

32 in B cell development and differentiation.

33 **Capsule summary**: Humoral immune defects are described in 9 patients from 5 families with

34 STK4 deficiency. A mouse <u>model</u> carrying the novel p.Y88del show that these defects are intrinsic

35 to the B cells.

36 **Key words:** STK4 deficiency; combined immunodeficiency disease; CRISPR/Cas9; mouse model;

37 humoral immunity; germinal centre; plasma cells; memory B cells.

38 **Abbreviations:** STK4, serine-threonine kinase 4; MST1, mammalian sterile 20-like 1; B_{mem},

39 memory B cells; GC, germinal centre; ASC, antibody-secreting cell; BCR, B cell receptor; HEL,

40 hen-egg lysozyme.

41

To the Editor:

Biallelic loss-of-function mutations in serine threonine kinase 4 (*STK4*), also known as mammalian sterile 20-like 1 (*MST1*), are associated with a combined immunodeficiency characterised by recurrent bacterial, fungal and viral infections (1-6). Most patients have intermittent neutropenia, T and B lymphopenia and, paradoxically, specific antibody defects despite the reported presence of elevated levels of serum IgG, A and E antibodies and antibody-mediated autoimmune cytopenias (1-6). While there have been numerous studies of neutrophil, macrophage, dendritic cell and T cell function in *Stk4* knock-out mice (7-11), the nature and basis of the underlying B cell dysregulation in STK4-deficient patients remains poorly characterised. To address this, we investigated the B cell phenotype and function in 9 patients from 5 unrelated families with *STK4* deficiency due to 5 different mutations, 2 of which are novel (Table E1 and Fig E1, A), and in CRISPR/Cas9 gene-edited mice carrying either the novel p.Y88del 3 base pair in-frame deletion (*Y88del*) in the kinase domain of STK4 present in 2 of these patients, or a premature stop codon (Fig E1, B-C). Notably, we did not observe elevated immunoglobulins, with the exception of IgE in our patients (Figure E1, D). Indeed, the dysglobulinemia in our STK4-deficient patients more closely resembles that observed in patients with DOCK8 deficiency.

STK4 protein expression was decreased in $Stk4^{Y88del/Y88del}$ and $Stk4^{-/-}$ mice (Fig E1, E), confirming the p.Y88del mutation affects protein stability, resulting in STK4 deficiency. $Stk4^{Y88del/Y88del}$ and $Stk4^{-/-}$ mice phenocopy the two patients with the mutation with elevated IgE and decreased peripheral blood naïve T cells (Table E1, Fig 1, A and E1, F-G). Immunization with sheep red blood cells (SRBCs) demonstrated that, similar to STK4-deficient patients, mice had specific antibody defects (Fig 1, B). STK4-deficient patients have decreased proportions of circulating memory B cells (B_{mems}) and increased transitional B cells compared to age-matched healthy controls (Fig 1, C and refs. 1-3, 5-6). Therefore, we examined B cell development in $Stk4^{Y88del/Y88del}$ mice. While early B cell development in the bone marrow was relatively normal (Fig E2, A), there was a decrease in the number of splenic mature follicular B cells, an absence of splenic marginal zone B cells, and a decrease in the proportion of peritoneal cavity B1a cells in $Stk4^{Y88del/Y88del}$ and $Stk4^{-/-}$ mice compared to WT mice (Fig 1, D-F), similar to observations made previously in other strains of *Stk4*-deficient mice (9, 12-14). Mixed bone marrow radiation chimeras demonstrated that these defects in peripheral B-cell differentiation were cell-intrinsic, and not secondary to T cell or myeloid cell defects (Fig E2, B-E).

Naïve B cells from STK4-deficient patients were cultured in vitro to determine their capacity to proliferate and differentiate into antibody-secreting cells (ASCs). This revealed a mild proliferative

3

defect in response to mimics of BCR engagement, but not T-cell help induced by CD40L and IL-21 (Fig 2, A). Interestingly, while naïve B cells from patients and healthy controls generated similar numbers of ASCs (Fig 2, B), STK4-deficient ASCs secreted less antibodies in response to CD40L and IL-21 stimulation (Fig 2, C). Notably, while CD19 expression has been reported to be reduced on B cells from *Stk4* knock-out mice (12), the level of CD19 was not found to be significantly decreased in both STK4-deficient patients and gene-targeted mice (Fig E3, A-B). Accordingly, there were no differences in BCR-mediated upregulation of CD69 and CD86 following in vitro stimulation with cognate antigen of STK4-deficient mouse B cells (Fig 2, D).

$Stk4^{Y88del/Y88del}$ mice were immunized with SRBCs and this showed a decreased number of germinal centre (GC) B cells, B_{mems} and plasma cells compared to $Stk4^{+/+}$ mice (Fig 2, E). STK4-deficient patients have decreased circulating memory Tfh cells (Fig E4, A), and immunized mice have decreased Tfh cells in the spleen (Fig E4, B). Mixed bone marrow chimeras suggested that, despite the Tfh cell defect in intact mice, the defective humoral immune response was B cell-intrinsic (Fig E4, C-E). This was confirmed by adoptive transfer experiments in which SW_{HEL} B cells (15) were used to track affinity maturation to cognate antigen (16). This showed that, in a system where the immune system was otherwise completely intact, while the response of STK4-gene-targeted SW_{HEL} B cells on day 5 was comparable to wild-type SW_{HEL} B cells, STK4 mutant SW_{HEL} B cells failed to expand and sustain the GC response, which rapidly contracted by day 9. Notably, there was also a relative reduction in the proportion of dark zone GC B cells (Fig 2, F and E5, A). Short-term labeling with BrdU showed that this failure to sustain the GC reaction was due to defective proliferation rather than increased cell death as there was no difference in caspase-3 staining (Fig 2, G and E5, B). Nevertheless, somatic hypermutation, affinity maturation, and class switch recombination were unaffected (Fig E5, C-D).

We next examined the capacity of SW_{HEL} B cells with STK4 mutations to differentiate into B_{mems} and plasma cells in vivo. Similar to immunization with SRBCs, there was defective generation of $Stk4^{Y88del/Y88del}$ B_{mems} (Fig 2, H). However, the residual $Stk4^{Y88del/Y88del}$ B_{mems} were functional, as shown by their ability to generate recall responses in immune mice, albeit to a greatly reduced extent compared to wild-type B_{mems} (Fig E6, A-C). Consistent with this, the few B_{mems} present in STK4-deficient patients were capable of differentiating into ASCs in vitro, albeit at reduced levels (Fig E6, D). Interestingly, despite the impaired specific antibody secretion in mice with $Stk4^{Y88del/Y88del}$ B cells, STK4 deficiency did not quantitatively impact the ability of these SW_{HEL} B cells to generate plasma cells in vivo (Fig 2, I-K). Thus, similar to B cells from STK4-deficient

4

112 patients, *Stk4^Y88del/Y88del* B cells are able to differentiate into plasma cells, but these plasma cells fail

113 to secrete adequate amounts of specific antibody.

114

115 STK4 is a multifunctional kinase that phosphorylates multiple cellular proteins, including those in

116 the Hippo signaling pathway (17, 18). Many of these substrates are also phosphorylated by its

117 paralog STK3, suggesting STK3 may functionally compensate for STK4 deficiency. Indeed, B cell

118 defects are more readily observed in *Stk3/Stk4* double knockout mice (14). Interestingly, STK4 has

119 been shown to phosphorylate FOXO1 and promote its nuclear localization (19), and FOXO1 was

120 recently shown to be is required for dark zone formation and GC maintenance (20-22). However,

121 while FOXO1 levels were decreased in *Stk4^Y88del/Y88del* and *Stk4^-/-* GC B cells, we could not rescue

122 the GC defect by retroviral overexpression of *Foxo1* (Fig E7, A-B), suggesting that other

123 mechanisms might also be involved. Another limitation of our study is the small number of patients

124 involved which prevents any firm conclusion, especially regarding differences in the serum

125 immunoglobulin levels in our cohort of 9 patients and the previously reported 14 patients.

126 Nevertheless, our data establishes a B cell-intrinsic requirement for STK4 in humoral immunity in

127 mice and humans.

128

131

132 *Imogen Moran, PhD[1,2]*

133 *Danielle T. Avery, BSc[1]*

134 *Kathryn Payne, BSc[1]*

135 *Helen Lenthall, MMSc[1]*

136 *E Graham Davies, MD[3]*

137 *Siobhan Burns, MD PhD[4,5]*

138 *Winnie Ip, MD[3]*

139 *Matÿfffedas M. Oleastro, MD[6]*

140 *Ismail Reisli, MD[7]*

141 *Sukru Guner, MD[7]*

142 *Sevgi Keles, MD[7]*

143 *Luigi Notarangelos, MD[8]*

144 *Elissa K. Deenick, PhD[1,2]*

145 *Christopher C Goodnow, PhD[1,2]*

146 *David Zahra, PhD[1]*

147 *Robert Brink, PhD[1,2]*

148 *CIRCA[9]*

149 *Melanie Wong, PhD[10,11*]*

150 *Stuart G. Tangye, PhD[1,2*]*

151 *Cindy S. Ma, PhD[1,2*]*

152 *Tri Giang Phan, PhD[1,2*]*

153

154 * Equal senior author

155 **From** [1]Immunology Division, Garvan Institute of Medical Research, Sydney, Australia; [2]St
156 Vincent's Clinical School, Faculty of Medicine, UNSW Sydney, Sydney, Australia; [3]Infection,
157 Immunity and Inflammation Theme, UCL Great Ormond Street Institute of Child Health, London,
158 United Kingdom; Department of Immunology, Great Ormond Street Hospital, London, United
159 Kingdom; [4]Department of Immunology, Royal Free London NHS Foundation Trust, London,
160 United Kingdom; [5]University College London, Institute of Immunity and Transplantation, London,
161 United Kingdom; [6]Immunology and Rheumatology Department, Hospital de Pediatría "Dr. Juan P.
162 Garrahan", Combate de los Pozos, 1881, Buenos Aires, Argentina; [7]Division of Pediatric
163 Immunology and Allergy, Meram Faculty of Medicine, Necmettin Erbakan University, Konya,
164 Turkey; [8]Laboratory of Clinical Immunology and Microbiology, National Institutes of Allergy and
165 Infectious Diseases, National Institutes of Health, Bethesda, Maryland, USA; [9]Clinical
166 Immunogenomics Research Consortium Australia; [10]Children's Hospital at Westmead, NSW,
167 Australia; [11]Faculty of Medicine, University of Sydney, Sydney, NSW, Australia.

168 **Correspondence:** Dr Tri Phan, t.phan@garvan.org.au

169

170 **References:**

171

172 1.   Abdollahpour H, Appaswamy G, Kotlarz D, Diestelhorst J, Beier R, Schäffer AA, et al. The
173 phenotype of human STK4 deficiency. *Blood*. 2012;119(15):3450-7.

174 2.   Nehme NT, Schmid JP, Debeurme F, André-Schmutz I, Lim A, Nitschke P, et al. MST1
175 mutations in autosomal recessive primary immunodeficiency characterized by defective naive T-
176 cell survival. *Blood*. 2012;119(15):3458-68.

177 3.   Halacli SO, Ayvaz DC, Sun-Tan C, Erman B, Uz E, Yilmaz DY, et al. STK4 (MST1)
178 deficiency in two siblings with autoimmune cytopenias: A novel mutation. *Clinical Immunology*.
179 2015;161(2):316-23.

180 4.   Crequer A, Picard C, Patin E, D'Amico A, Abhyankar A, Munzer M, et al. Inherited MST1
181 Deficiency Underlies Susceptibility to EV-HPV Infections. *PLOS ONE*. 2012;7(8):e44010.

182   5.   Dang TS, Willet JDP, Griffin HR, Morgan NV, O'Boyle G, Arkwright PD, et al. Defective
183   Leukocyte Adhesion and Chemotaxis Contributes to Combined Immunodeficiency in Humans with
184   Autosomal Recessive MST1 Deficiency. *Journal of Clinical Immunology*. 2016;36(2):117-22.

185   6.   Schipp C, Fischer U, Schlütermann D, Hönscheid A, Nabhani S, Höll J, et al. EBV Negative
186   Lymphoma and Autoimmune Lymphoproliferative Syndrome Like Phenotype Extend the Clinical
187   Spectrum of Primary Immunodeficiency Caused by STK4 Deficiency. *Frontiers in Immunology*.
188   2018;9

189   7.   Kurz AR, Pruenster M, Rohwedder I, Ramadass M, Schafer K, Harrison U, et al. MST1-
190   dependent vesicle trafficking regulates neutrophil transmigration through the vascular basement
191   membrane. *J Clin Invest*. 2016;126(11):4125-39.

192   8.   Li C, Bi Y, Li Y, Yang H, Yu Q, Wang J, et al. Dendritic cell MST1 inhibits Th17
193   differentiation. *Nat Commun*. 2017;8:14275.

194   9.   Katagiri K, Katakai T, Ebisuno Y, Ueda Y, Okada T, Kinashi T. Mst1 controls lymphocyte
195   trafficking and interstitial motility within lymph nodes. *EMBO J*. 2009;28(9):1319-31.

196

1 **Title page:**

2 **B cell-intrinsic requirement for STK4 in humoral immunity in mice and humans**

3 *Imogen Moran, PhD[1,2], Danielle T. Avery, BSc[1], Kathryn Payne, BSc[1], Helen Lenthall, MMSc[1], E.*

4 *Graham Davies, MD[3], Siobhan Burns, MD PhD[4,5], Winnie Ip, MD[3], Matÿfffedas M. Oleastro, MD[6],*

5 *Ismail Reisli, MD[7], Sukru Guner, MD[7], Sevgi Keles, MD[7], Luigi Notarangelo, MD[8], Elissa K.*

6 *Deenick, PhD[1,2], Christopher C. Goodnow, PhD[1,2], David Zahra, PhD[1], Robert Brink, PhD[1,2],*

7 *CIRCA[9], Melanie Wong, PhD[10,11*], Stuart G. Tangye, PhD[1,2*], Cindy S. Ma, PhD[1,2*], Tri Giang*

8 *Phan, PhD[1,2*]*

9 * Equal senior author

10 **From** [1]Immunology Division, Garvan Institute of Medical Research, Sydney, Australia; [2]St

11 Vincent's Clinical School, Faculty of Medicine, UNSW Sydney, Sydney, Australia; [3]Infection,

12 Immunity and Inflammation Theme, UCL Great Ormond Street Institute of Child Health, London,

13 United Kingdom; Department of Immunology, Great Ormond Street Hospital, London, United

14 Kingdom; [4]Department of Immunology, Royal Free London NHS Foundation Trust, London,

15 United Kingdom; [5]University College London, Institute of Immunity and Transplantation, London,

16 United Kingdom; [6]Immunology and Rheumatology Department, Hospital de Pediatría "Dr. Juan P.

17 Garrahan", Combate de los Pozos, 1881, Buenos Aires, Argentina; [7]Division of Pediatric

18 Immunology and Allergy, Meram Faculty of Medicine, Necmettin Erbakan University, Konya,

19 Turkey; [8]Laboratory of Clinical Immunology and Microbiology, National Institutes of Allergy and

20 Infectious Diseases, National Institutes of Health, Bethesda, Maryland, USA; [9]Clinical

21 Immunogenomics Research Consortium Australia; [10]Children's Hospital at Westmead, NSW,

22 Australia; [11]Faculty of Medicine, University of Sydney, Sydney, NSW, Australia.

23 **Correspondence:** Dr Tri Phan; Address: Garvan Institute of Medical Research, 384 Victoria St

24 Darlinghurst NSW Australia; Telephone: +61 2 92958414; Facsimile: +61 2 92958404; Email:

25 t.phan@garvan.org.au .

30 **Conflicts of interest:** The authors have no conflicts of interest to declare.

31 **Key finding:** Patients with STK4 deficiency have humoral immune defects due to intrinsic defects

32 in B cell development and differentiation.

33 **Capsule summary**: Humoral immune defects are described in 9 patients from 5 families with

34 STK4 deficiency. A mouse model carrying the novel p.Y88del show that these defects are intrinsic

35 to the B cells.

36 **Key words:** STK4 deficiency; combined immunodeficiency disease; CRISPR/Cas9; mouse model;

37 humoral immunity; germinal centre; plasma cells; memory B cells.

38 **Abbreviations:** STK4, serine-threonine kinase 4; MST1, mammalian sterile 20-like 1; B_{mem},

39 memory B cells; GC, germinal centre; ASC, antibody-secreting cell; BCR, B cell receptor; HEL,

40 hen-egg lysozyme.

41

To the Editor:

Biallelic loss-of-function mutations in serine threonine kinase 4 (*STK4*), also known as mammalian sterile 20-like 1 (*MST1*), are associated with a combined immunodeficiency characterised by recurrent bacterial, fungal and viral infections (1-6). Most patients have intermittent neutropenia, T and B lymphopenia and, paradoxically, specific antibody defects despite the reported presence of elevated levels of serum IgG, A and E antibodies and antibody-mediated autoimmune cytopenias (1-6). While there have been numerous studies of neutrophil, macrophage, dendritic cell and T cell function in *Stk4* knock-out mice (7-11), the nature and basis of the underlying B cell dysregulation in STK4-deficient patients remains poorly characterised. To address this, we investigated the B cell phenotype and function in 9 patients from 5 unrelated families with *STK4* deficiency due to 5 different mutations, 2 of which are novel (Table E1 and Fig E1, A), and in CRISPR/Cas9 gene-edited mice carrying either the novel p.Y88del 3 base pair in-frame deletion (*Y88del*) in the kinase domain of STK4 present in 2 of these patients, or a premature stop codon (Fig E1, B-C). Notably, we did not observe elevated immunoglobulins, with the exception of IgE in our patients (Figure E1, D). Indeed, the dysglobulinemia in our STK4-deficient patients more closely resembles that observed in patients with DOCK8 deficiency.

STK4 protein expression was decreased in $Stk4^{Y88del/Y88del}$ and $Stk4^{-/-}$ mice (Fig E1, E), confirming the p.Y88del mutation affects protein stability, resulting in STK4 deficiency. $Stk4^{Y88del/Y88del}$ and $Stk4^{-/-}$ mice phenocopy the two patients with the mutation with elevated IgE and decreased peripheral blood naïve T cells (Table E1, Fig 1, A and E1, F-G). Immunization with sheep red blood cells (SRBCs) demonstrated that, similar to STK4-deficient patients, mice had specific antibody defects (Fig 1, B). STK4-deficient patients have decreased proportions of circulating memory B cells (B_{mems}) and increased transitional B cells compared to age-matched healthy controls (Fig 1, C and refs. 1-3, 5-6). Therefore, we examined B cell development in $Stk4^{Y88del/Y88del}$ mice. While early B cell development in the bone marrow was relatively normal (Fig E2, A), there was a decrease in the number of splenic mature follicular B cells, an absence of splenic marginal zone B cells, and a decrease in the proportion of peritoneal cavity B1a cells in $Stk4^{Y88del/Y88del}$ and $Stk4^{-/-}$ mice compared to WT mice (Fig 1, D-F), similar to observations made previously in other strains of *Stk4*-deficient mice (9, 12-14). Mixed bone marrow radiation chimeras demonstrated that these defects in peripheral B-cell differentiation were cell-intrinsic, and not secondary to T cell or myeloid cell defects (Fig E2, B-E).

Naïve B cells from STK4-deficient patients were cultured in vitro to determine their capacity to proliferate and differentiate into antibody-secreting cells (ASCs). This revealed a mild proliferative

3

defect in response to mimics of BCR engagement, but not T-cell help induced by CD40L and IL-21 (Fig 2, A). Interestingly, while naïve B cells from patients and healthy controls generated similar numbers of ASCs (Fig 2, B), STK4-deficient ASCs secreted less antibodies in response to CD40L and IL-21 stimulation (Fig 2, C). Notably, while CD19 expression has been reported to be reduced on B cells from *Stk4* knock-out mice (12), the level of CD19 was not found to be significantly decreased in both STK4-deficient patients and gene-targeted mice (Fig E3, A-B). Accordingly, there were no differences in BCR-mediated upregulation of CD69 and CD86 following in vitro stimulation with cognate antigen of STK4-deficient mouse B cells (Fig 2, D).

Stk4$^{Y88del/Y88del}$ mice were immunized with SRBCs and this showed a decreased number of germinal centre (GC) B cells, B$_{mems}$ and plasma cells compared to *Stk4*$^{+/+}$ mice (Fig 2, E). STK4-deficient patients have decreased circulating memory Tfh cells (Fig E4, A), and immunized mice have decreased Tfh cells in the spleen (Fig E4, B). Mixed bone marrow chimeras suggested that, despite the Tfh cell defect in intact mice, the defective humoral immune response was B cell-intrinsic (Fig E4, C-E). This was confirmed by adoptive transfer experiments in which SW$_{HEL}$ B cells (15) were used to track affinity maturation to cognate antigen (16). This showed that, in a system where the immune system was otherwise completely intact, while the response of STK4-gene-targeted SW$_{HEL}$ B cells on day 5 was comparable to wild-type SW$_{HEL}$ B cells, STK4 mutant SW$_{HEL}$ B cells failed to expand and sustain the GC response, which rapidly contracted by day 9. Notably, there was also a relative reduction in the proportion of dark zone GC B cells (Fig 2, F and E5, A). Short-term labeling with BrdU showed that this failure to sustain the GC reaction was due to defective proliferation rather than increased cell death as there was no difference in caspase-3 staining (Fig 2, G and E5, B). Nevertheless, somatic hypermutation, affinity maturation, and class switch recombination were unaffected (Fig E5, C-D).

We next examined the capacity of SW$_{HEL}$ B cells with STK4 mutations to differentiate into B$_{mems}$ and plasma cells in vivo. Similar to immunization with SRBCs, there was defective generation of *Stk4*$^{Y88del/Y88del}$ B$_{mems}$ (Fig 2, H). However, the residual *Stk4*$^{Y88del/Y88del}$ B$_{mems}$ were functional, as shown by their ability to generate recall responses in immune mice, albeit to a greatly reduced extent compared to wild-type B$_{mems}$ (Fig E6, A-C). Consistent with this, the few B$_{mems}$ present in STK4-deficient patients were capable of differentiating into ASCs in vitro, albeit at reduced levels (Fig E6, D). Interestingly, despite the impaired specific antibody secretion in mice with *Stk4*$^{Y88del/Y88del}$ B cells, STK4 deficiency did not quantitatively impact the ability of these SW$_{HEL}$ B cells to generate plasma cells in vivo (Fig 2, I-K). Thus, similar to B cells from STK4-deficient

4

112 patients, *Stk4*[Y88del/Y88del] B cells are able to differentiate into plasma cells, but these plasma cells fail

113 to secrete adequate amounts of specific antibody.

114

115 STK4 is a multifunctional kinase that phosphorylates multiple cellular proteins, including those in

116 the Hippo signaling pathway (17, 18). Many of these substrates are also phosphorylated by its

117 paralog STK3, suggesting STK3 may functionally compensate for STK4 deficiency. Indeed, B cell

118 defects are more readily observed in *Stk3/Stk4* double knockout mice (14). Interestingly, STK4 has

119 been shown to phosphorylate FOXO1 and promote its nuclear localization (19), and FOXO1 was

120 recently shown to be is required for dark zone formation and GC maintenance (20-22). However,

121 while FOXO1 levels were decreased in *Stk4*[Y88del/Y88del] and *Stk4*^{-/-} GC B cells, we could not rescue

122 the GC defect by retroviral overexpression of *Foxo1* (Fig E7, A-B), suggesting that other

123 mechanisms might also be involved. Another limitation of our study is the small number of patients

124 involved which prevents any firm conclusion, especially regarding differences in the serum

125 immunoglobulin levels in our cohort of 9 patients and the previously reported 14 patients.

126 Nevertheless, our data establishes a B cell-intrinsic requirement for STK4 in humoral immunity in

127 mice and humans.

128

131

132 *Imogen Moran, PhD*[1,2]

133 *Danielle T. Avery, BSc*[1]

134 *Kathryn Payne, BSc*[1]

135 *Helen Lenthall, MMSc*[1]

136 *E Graham Davies, MD*[3]

137 *Siobhan Burns, MD PhD*[4,5]

138 *Winnie Ip, MD*[3]

139 *Matÿfffedas M. Oleastro, MD*[6]

140 *Ismail Reisli, MD*[7]

141 *Sukru Guner, MD*[7]

142 *Sevgi Keles, MD*[7]

143 *Luigi Notarangelos, MD*[8]

144 *Elissa K. Deenick, PhD*[1,2]

145 *Christopher C Goodnow, PhD*[1,2]

146 *David Zahra, PhD*[1]

5

147   *Robert Brink, PhD[1,2]*

148   *CIRCA[9]*

149   *Melanie Wong, PhD[10,11*]*

150   *Stuart G. Tangye, PhD[1,2*]*

151   *Cindy S. Ma, PhD[1,2*]*

152   *Tri Giang Phan, PhD[1,2*]*

153

154   * Equal senior author

155   **From** [1]Immunology Division, Garvan Institute of Medical Research, Sydney, Australia; [2]St

156   Vincent's Clinical School, Faculty of Medicine, UNSW Sydney, Sydney, Australia; [3]Infection,

157   Immunity and Inflammation Theme, UCL Great Ormond Street Institute of Child Health, London,

158   United Kingdom; Department of Immunology, Great Ormond Street Hospital, London, United

159   Kingdom; [4]Department of Immunology, Royal Free London NHS Foundation Trust, London,

160   United Kingdom; [5]University College London, Institute of Immunity and Transplantation, London,

161   United Kingdom; [6]Immunology and Rheumatology Department, Hospital de Pediatría "Dr. Juan P.

162   Garrahan", Combate de los Pozos, 1881, Buenos Aires, Argentina; [7]Division of Pediatric

163   Immunology and Allergy, Meram Faculty of Medicine, Necmettin Erbakan University, Konya,

164   Turkey; [8]Laboratory of Clinical Immunology and Microbiology, National Institutes of Allergy and

165   Infectious Diseases, National Institutes of Health, Bethesda, Maryland, USA; [9]Clinical

166   Immunogenomics Research Consortium Australia; [10]Children's Hospital at Westmead, NSW,

167   Australia; [11]Faculty of Medicine, University of Sydney, Sydney, NSW, Australia.

168   **Correspondence:** Dr Tri Phan, t.phan@garvan.org.au

169

170   **References:**

171

172   1.   Abdollahpour H, Appaswamy G, Kotlarz D, Diestelhorst J, Beier R, Schäffer AA, et al. The

173   phenotype of human STK4 deficiency. *Blood*. 2012;119(15):3450-7.

174   2.   Nehme NT, Schmid JP, Debeurme F, André-Schmutz I, Lim A, Nitschke P, et al. MST1

175   mutations in autosomal recessive primary immunodeficiency characterized by defective naive T-

176   cell survival. *Blood*. 2012;119(15):3458-68.

177   3.   Halacli SO, Ayvaz DC, Sun-Tan C, Erman B, Uz E, Yilmaz DY, et al. STK4 (MST1)

178   deficiency in two siblings with autoimmune cytopenias: A novel mutation. *Clinical Immunology*.

179   2015;161(2):316-23.

180   4.   Crequer A, Picard C, Patin E, D'Amico A, Abhyankar A, Munzer M, et al. Inherited MST1

181   Deficiency Underlies Susceptibility to EV-HPV Infections. *PLOS ONE*. 2012;7(8):e44010.

182 5.   Dang TS, Willet JDP, Griffin HR, Morgan NV, O'Boyle G, Arkwright PD, et al. Defective
183 Leukocyte Adhesion and Chemotaxis Contributes to Combined Immunodeficiency in Humans with
184 Autosomal Recessive MST1 Deficiency. *Journal of Clinical Immunology*. 2016;36(2):117-22.

185 6.   Schipp C, Fischer U, Schlütermann D, Hönscheid A, Nabhani S, Höll J, et al. EBV Negative
186 Lymphoma and Autoimmune Lymphoproliferative Syndrome Like Phenotype Extend the Clinical
187 Spectrum of Primary Immunodeficiency Caused by STK4 Deficiency. *Frontiers in Immunology*.
188 2018;9

189 7.   Kurz AR, Pruenster M, Rohwedder I, Ramadass M, Schafer K, Harrison U, et al. MST1-
190 dependent vesicle trafficking regulates neutrophil transmigration through the vascular basement
191 membrane. *J Clin Invest*. 2016;126(11):4125-39.

192 8.   Li C, Bi Y, Li Y, Yang H, Yu Q, Wang J, et al. Dendritic cell MST1 inhibits Th17
193 differentiation. *Nat Commun*. 2017;8:14275.

194 9.   Katagiri K, Katakai T, Ebisuno Y, Ueda Y, Okada T, Kinashi T. Mst1 controls lymphocyte
195 trafficking and interstitial motility within lymph nodes. *EMBO J*. 2009;28(9):1319-31.

196

Moran et al_Figure 1_2018
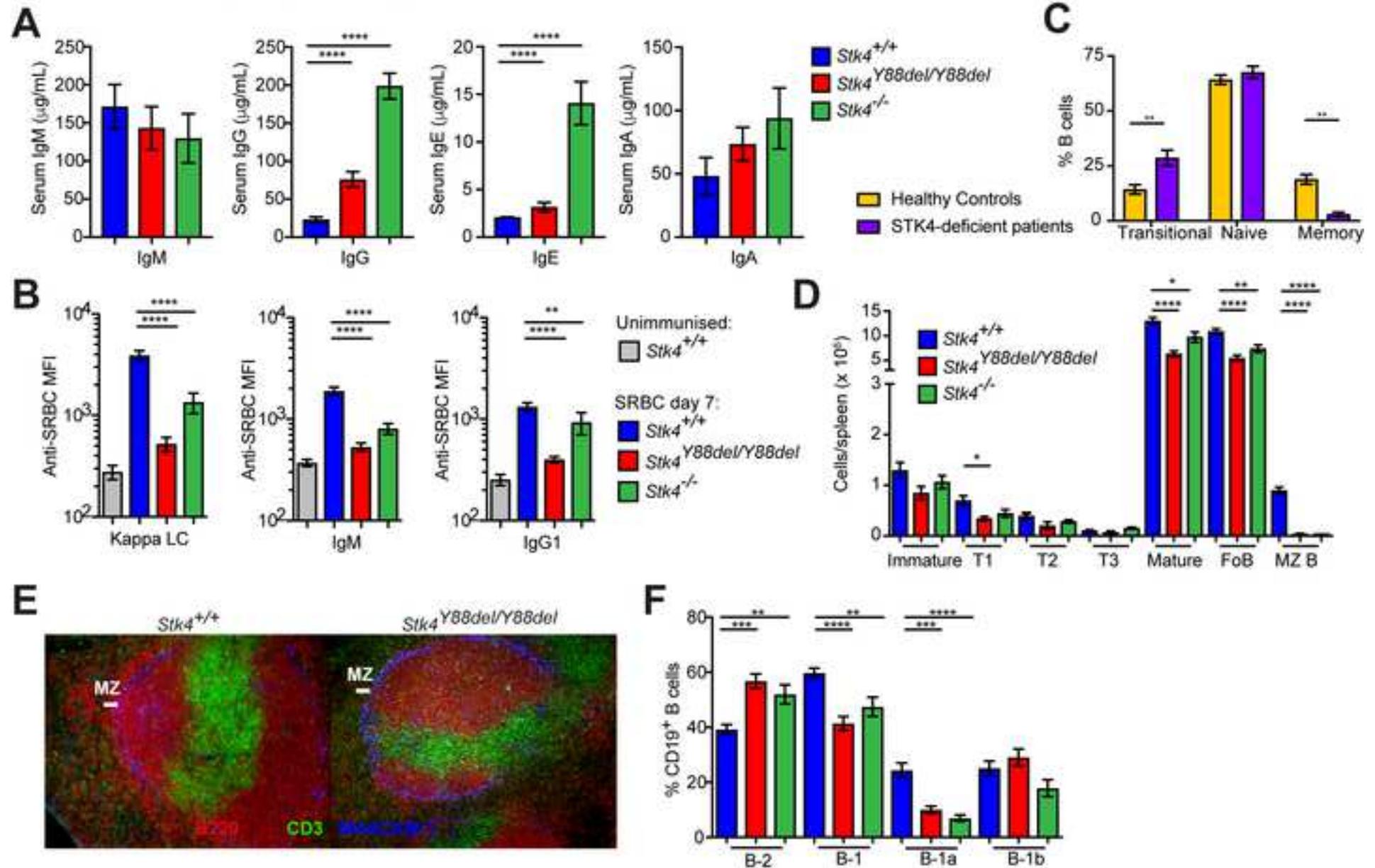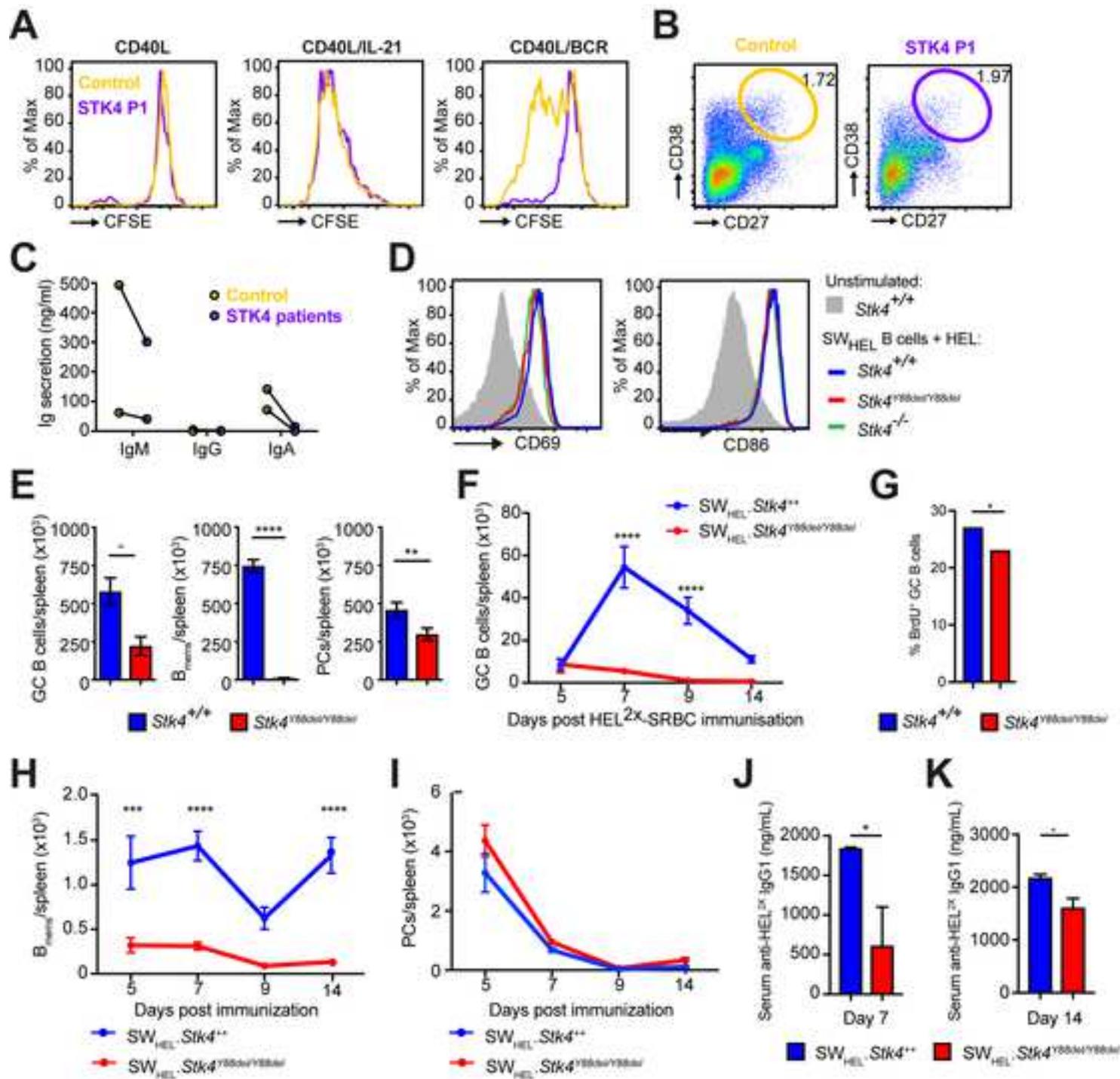
Patient	P1 (Family 1)	P2 (Family 1)	P3 (Family 2)	P4 (Family 2)	P5 (Family 3)	P6 (Family 3)	P7 (Family 4)	P8 (Family 5)	P9 (Family 5)
Country	Australia	Australia	England	England	Turkey	Turkey	Turkey	Argentian	Argentina
Genetics	homozygous	homozygous	homozygous	homozygous	homozygous	homozygous	homozygous	homozygous	homozygous
Mutation	p.Y88del		c.349C>T; p.R117X		c.1245delA; p.P416Lfs*4		c.1103delT; p.M368fsX369	c.343C>T; p.R115*	
Consanguinity	yes	yes	yes	yes	yes	yes	yes	no	no
Demographic	15M	10F	15F	21M	12M	14F	8F	4F	16M
Clinical features									
Eczema and skin infections	yes	yes	yes	yes	yes	yes	yes	no	no
Recurrent sinopulmonary infection	no	yes	yes	yes	yes	yes	yes	no	no
Oral candidiasis	no	no	no	yes	no	yes	no	no	no
Staphylococcal pneumonia	yes	no	no	no	no	no	no	no	no
Cryptoporidiosis	no	no	no	no	no	no	no	no	no
Allergic disease	no	yes	no	yes	yes	yes	no	no	no
Viral infections									
EBV	yes	no	yes	yes	no	no	no	yes	no
CMV	yes	no	no	no	no	no	no	no	no
Molluscum contagiosum	yes	yes	yes	yes	no	no	no	no	no
Varicella zoster virus (VZV)	yes	yes	no	yes	no	no	no	no	yes - encephalitis
Influenza	no	yes	no	no	no	no	no	no	no
Herpes simplex virus (HSV)	no	yes	no	no	yes	yes	yes	no	no
Human papillomavirus (HPV)	no	yes	no	no	no	no	no	no	yes
Autoimmunity									
ITP	yes	no	no	no	no	no	no	no	no
AIHA	yes	no	no	no	no	no	no	yes	yes
Other	no	no	no	no	no	no	no	no	no
Immunophenotyping (cells/mL)									
Total lymphocyte count	0.1	0.5	1.84	0.87	0.7	0.8	1.003	1.3	1.33
Total T cells	0.05	0.22	1.23	0.53	0.415	0.512	0.403	0.351	1.004
CD4 T cells	0.03	0.16	0.2	0.17	0.147	0.158	0.13	0.156	0.401
Naïve CD4 T cells	ND	ND	0.01	0.04	0.0966	0.0688	0.081	0.032	0.12
CD8 T cells	0.02	0.1	0.79	0.33	0.203	0.296	0.247	0.169	0.575
Naïve CD8 T cells	ND	ND	0.06	0.09	0.558	0.408	0.47	0.063	ND
B cells	0.1	0.2	0.39	0.18	0.14	0.144	0.388	0.806	0.228
Transitional B cells (% B cells)	ND	ND	17	13	25	36.5	8.5	ND	ND
Memory B cells (% B cells)	ND	ND	0.8	7	8.8	3	1.3	ND	0.147
Neutrophils	0.1	3	4.27	2.4	1.4	4.1	3.2	ND	1276
NK cells	0.04	0.06	0.18	0.06	0.077	0.144	0.265	0.074	0.08
Serum Ig levels									
IgG (g/L)	15	10	14.6	13.6	1.29	1.32	2.39	1.32	2.77
IgA (g/L)	3.5	7	0.151	0.112	0.272	0.215	0.34	0.039	0.738
IgM (g/L)	1.2	0.5	0.159	0.1	0.111	0.081	0.177	0.277	0.064
IgE (IU/L)	283	480	ND	ND	1280	569	1600	ND	1700
Specific antibody responses									
Pneumococcus	poor	intact	intact	no response	low	intact	intact	poor	absent
Tetanus toxoid	intact	intact	intact	no response	intact	poor	intact	poor	absent
Hemophilus	intact	intact	ND	ND	ND	ND	ND	ND	ND
Diphtheria toxin	intact	intact	ND	ND	ND	ND	ND	ND	ND
Isohemagglutinin	ND	ND	ND	ND	present	present	present	absent	absent
Hepatitis B surface antigen	intact	intact	ND	ND	absent	absent	absent	absent	absent
Treatment	HSCT	HSCT	IVIG	IVIG	SCIG	SCIG	SCIG	IVIG	IVIG

| IVIG pre-transplant | | Bactrim and fungal prophylaxis | Bactrim and fungal prophylaxis | Bactrim and fungal prophylaxis | Bactrim prophyaxis | Bactrim prophylaxis |

JACI-D-19-00027, B cell-intrinsic requirement for STK4 in humoral immunity in mice and humans

Figure Legends

Figure 1. STK4-deficient mice and patients have B cell-intrinsic defects in peripheral B cell development. (A) Serum immunoglobulins in unimmunized $Stk4^{Y88del/Y88del}$, $Stk4^{-/-}$ and $Stk4^{+/+}$ mice. Data are representative of >2 independent experiments with 7 mice per group. **(B)** Serum kappa light chain (LC), IgG1 and IgM antibodies against SRBCs 7 days after immunization. Data are representative of 2 independent experiments with 3-4 mice per group. **(C)** Proportion of circulating transitional, naïve and memory B cells in the peripheral blood of STK4-deficient patients and healthy donors. **(D)** Number of immature, transitional (T1-T3), mature, follicular (FoB) and marginal zone B cells (MZ B) in the spleen of $Stk4^{Y88del/Y88del}$, $Stk4^{-/-}$ and $Stk4^{+/+}$ mice. Combined data from 2 independent experiments with 4-5 mice per group. **(E)** Immunohistochemistry showing MAdCAM (blue), B220 (red) and CD3 (green) in splenic sections from $Stk4^{Y88del/Y88del}$ and $Stk4^{+/+}$ mice. Data are representative of 3 independent experiments with 2 mice per group. **(F)** Proportion of B-2, B-1, B-1a and B-1b cells in the peritoneum of $Stk4^{Y88del/Y88del}$, $Stk4^{-/-}$ and $Stk4^{+/+}$ mice. Data are combined from 2 independent experiments with 4-5 mice per group. ** $p < 0.01$, ****$p < 0.0001$.

Figure 2. STK4-deficient mice and patients have B cell-intrinsic defects in humoral immunity. Naïve B cells from STK4-deficient patients and healthy controls were sorted and cultured in vitro to assess **(A)** CFSE dilution, **(B)** plasma cell differentiation, and **(C)** immunoglobulin secretion after 4-5 days. **(D)** B cells from from $Stk4^{Y88del/Y88del}$, $Stk4^{-/-}$ and $Stk4^{+/+}$ SW_{HEL} mice were stimulated overnight to assess BCR signaling. **(E)** Humoral immune response in $Stk4^{Y88del/Y88del}$ and $Stk4^{+/+}$ mice immunized 7 days earlier with SRBC. **(F)** Kinetics of the GC B cell response of adoptively transferred $Stk4^{Y88del/Y88del}$ and $Stk4^{+/+}$ SW_{HEL} B cells. **(G)** Decreased proliferation of $Stk4^{Y88del/Y88del}$ compared to $Stk4^{+/+}$ SW_{HEL} GC B cells. Data combined from 2 independent experiments with 4-5 mice per group on day 5. Kinetics of **(H)** B_{mems} and **(I)** plasma cell response of adoptively transferred $Stk4^{+/+}$ or $Stk4^{Y88del/Y88del}$ SW_{HEL} B cells. **(J)** Serum anti-HEL (total) antibodies on 7 day and **(K)** anti-HEL^{2X} (high affinity) antibodies on 14 day. Unless otherwise stated, mouse data is representative of at least 2 independent experiments with >4 mice per group per time point. * $p < 0.5$, *** $p < 0.001$, ****$p < 0.0001$.

Table E1. Clinical phenotype and laboratory findings in 9 STK4-deficient patients from 5 families.

Extended figure legends

Figure E1. Mutations in a cohort of 8 patients with STK4 deficiency and generation of a novel mouse model of STK4 deficiency. (A) Model of STK4 protein showing position of known mutations in STK4-deficient patients. Novel Y88del and R115* mutations in this report are shown in red; previously described mutations are in black. *AID*, autoinhibitory domain; *SARAH*, Sav/Rassf/Hpo domain. **(B)** Model of STK4 showing position of Y88 residue in the ATP binding site. **(C)** Generation of CRISPR/Cas9 gene-edited mice with deletion of the Y88 amino acid residue ($Stk4^{Y88del/Y88del}$) or a knockout with a premature stop codon ($Stk4^{-/-}$). **(D)** Serum immunoglobulin levels and age-matched reference ranges (grey shading) of 9 patients with STK4 deficiency. **(E)** Western blot STK4 protein levels in $Stk4^{+/+}$, $Stk4^{Y88del/Y88del}$ and $Stk4^{-/-}$ murine splenocytes. **(F)** Proportion of naïve, effector memory and central memory CD4 and CD8 T cells in peripheral blood of healthy donors or STK4-deficient patients. **(G)** Proportion of naïve, effector memory and central memory CD4 and CD8 T cells in peripheral blood of $Stk4^{Y88del/Y88del}$, $Stk4^{-/-}$ and $Stk4^{+/+}$ mice. Data representative of 2 independent experiments with 4-5 mice per group. * $p < 0.05$, ** $p < 0.01$, *** $p < 0.001$, ****$p < 0.0001$.

Figure E2. B cell-intrinsic defect in peripheral B cell development in STK4 deficient mice. (A) Number of pre-pro, pro, pre, immature and mature B cells in the bone marrow of $Stk4^{Y88del/Y88del}$, $Stk4^{-/-}$ and $Stk4^{+/+}$ mice. Data are combined from 2 independent experiments with 4-5 mice per group. **(B)** Experimental design of mixed bone marrow radiation chimera mice that were reconstituted with 50% CD45.1$^+$ $Stk4^{+/+}$ and 50% CD45.2$^+$ $Stk4^{Y88del/Y88del}$ or $Stk4^{+/+}$ bone marrow. Reconstitution ratios of B cell subsets in **(C)** bone marrow, **(D)** spleen and **(E)** peritoneal cavity of mixed chimera mice with 50% CD45.1$^+$ $Stk4^{+/+}$ and 50% CD45.2$^+$ $Stk4^{Y88del/Y88del}$ or $Stk4^{+/+}$. Data are combined from 2 independent experiments with 3-6 mice per group. *** $p < 0.001$, ****$p < 0.0001$.

Figure E3. Normal expression of CD19 in human and mouse STK4 deficient B cells. (A) Expression of BCR co-receptor CD19 on human peripheral blood B cell subsets from healthy donors and STK4 deficient patients. **(B)** Expression of BCR co-receptor CD19 on splenic B cells $Stk4^{Y88del/Y88del}$, $Stk4^{-/-}$ and $Stk4^{+/+}$ mice. Data representative of 3 independent experiments with >3 mice per group. * $p < 0.05$.

Figure E4. B cell-intrinsic defect in humoral immune response. (A) Measurement of circulating memory Tfh cells in the blood of STK4-deficient patients. **(B)** Tfh cell numbers in the spleen of STK4-deficient mice on day 7 after SRBC immunization. Reconstitution ratios on day 7 of SRBC immunization in spleen for **(B)** GC B cells, **(C)** B$_{mems}$ and **(D)** plasma cells of mixed chimera mice

with input of 50% CD45.1[+] *Stk4*^{+/+} and 50% CD45.2[+] *Stk4*[Y88del/Y88del] or *Stk4*^{+/+}. Data are representative of 2 independent experiments with 3-6 mice per group. ****$p < 0.0001$.

Figure E5. Altered composition of the GC but normal cell death, somatic hypermutation and class switching in STK4-deficient B cells. (A) Proportion of dark zone (DZ) and light zone (LZ) GC B cells from day 7 of *Stk4*^{+/+} or *Stk4*[Y88del/Y88del] SW$_{HEL}$ B HEL[2X]-SRBC response. Data are representative of 2 independent experiments with 5 mice per group. **(B)** Proportion of active caspase-3 cells in the GC in mice adoptively transferred with *Stk4*^{+/+} or *Stk4*[Y88del/Y88del] SW$_{HEL}$ B cells challenged with HEL[2X]-SRBC. Data is combined from 2 independent experiments with 4-5 mice per group on day 5. **(C)** Sequencing analysis of Ig heavy chain genes showing proportion of GC B cells with affinity increasing mutations, including the canonical Y53D mutation, in mice adoptively transferred with *Stk4*^{+/+} or *Stk4*[Y88del/Y88del] SW$_{HEL}$ B cells challenged with HEL[3X]-SRBC. n shows number of GC B cells sequenced and number mutations/cells shows total number of mutations in sequenced region. Representative of 2 independent experiments with 4 -5 mice per group. **(D)** Proportion of IgG1^{+} B cells in the GC in mice adoptively transferred with *Stk4*^{+/+} or *Stk4*[Y88del/Y88del] SW$_{HEL}$ B cells challenged with HEL[3X]-SRBC. Data are representative of 2 independent experiments with 5 mice per group per time point. *** $p < 0.001$

Figure E6. Memory B cells were functional and able to generate a secondary response. (A) Experimental design to setup a B$_{mem}$ lymph node response, where *Stk4*^{+/+} or *Stk4*[Y88del/Y88del] SW$_{HEL}$ B cells and wild-type OT2 CD4 T cells were adoptively transferred into recipient mice and challenged with HEL-OVA. **(B)** Number of donor (CD45.1[+]) B$_{mems}$ in draining lymph node. **(C)** Number of donor B cells in the recall response in draining lymph node. Lymph node data are representative of 2 independent experiments with 4-5 mice per group per time point. **(D)** Immunoglobulin secretion of cultured sorted memory B cells from STK4-deficient patients and healthy donors. * $p < 0.5$, ****$p < 0.0001$.

Figure E7. STK4 deficiency results in decreased FOXO1 expression but overexpression of FOXO1 does not rescue germinal centre defect. (A) Intracellular FACS analysis of FOXO1 expression in GC B cells and total B cells 7 days after SRBC immunization of *Stk4*[Y88del/Y88del], *Stk4*^{-/-} and *Stk4*^{+/+} mice. **(B)** Proportion of donor lymphocytes following retroviral overexpression in mice adoptively transferred with *Stk4*^{+/+} or *Stk4*[Y88del/Y88del] SW$_{HEL}$ B cells challenged with HEL[3X]-SRBC. All data are representative of 2 independent experiments with 3-4 mice per group per time point. **$p < 0.01$, ****$p < 0.0001$.

METHODS

Human blood samples

Buffy coats from healthy donors were purchased from the Australian Red Cross Blood Service. Pediatric blood samples were collected from individuals either attending clinic for non-immunological conditions, or for genetic testing due to a family history of disease, but were found not to carry the mutation. Whole blood was collected, PBMCs were isolated and cryopreserved as single-cell suspensions, shipped to the Garvan Institute on dry ice, and then stored in liquid nitrogen until use. Approval for this study was obtained from the relevant hospital human research ethics committees. Informed consent was obtained from all participants for human experiments described in this study.

Human lymphocyte phenotyping

PBMCs were incubated with following mAbs: BUV395-anti CD20, PE-Cy7-anti CD27, BV786-anti CD27, APC-anti CD10, BV421-anti CD3, BUV737-anti CD4, BUV395-anti CD8, PE-Cy7-anti CCR7, BV605-anti CD45RA, APC-anti CD38, BV711-anti CD19. The proportions of $CD20^+$ $CD27^-$ $CD10^+$ (transitional), $CD20^+$ $CD27^-$ $CD10^-$ (naïve), and $CD20^+$ $CD27^+$ $CD10^-$ (memory) B cells, and T cell subsets (CD4 or CD8) naïve ($CCR7^+$ $CD45RA^+$), central memory ($CCR7^+$ $CD45RA^-$), effector memory ($CCR7^-$ $CD45RA^-$) and for $CD8^+$ cells terminally differentiated effector memory T cells expressing CD45RA ($CCR7^-$ $CD45RA^+$) was determined by flow cytometry (LSRII, Becton Dickinson) and analysed using FlowJo software (Tree Star).

Isolation and in vitro activation of human B cell subsets

PBMCs were labeled with mAbs against CD20, CD27, and CD10 and naïve ($CD20^+$ $CD10^-$ $CD27^-$) B cells were then sorted using a FACS Aria III (Becton Dickinson). Purity of the recovered populations was >90%. Naïve B cells were then cultured as previously described (23). B cell viability was determined using the Zombie Aqua Viability dye (BioLegend) and proliferation determined by CFSE (eBioscience) dilution after 4-5d of in vitro culture. Differentiation of B cells to plasmablasts was assessed by determining the frequency of naïve B cells acquiring a $CD38^{hi}$ $CD27^{hi}$ phenotype during in vitro culture by flow cytometry (LSRII, Becton Dickinson) and analyzed using FlowJo software (Tree Star).

Human Ig ELISAs

Secretion of IgM, IgG and IgA by in vitro cultured human transitional and naive B cells was

determined using Ig heavy-chain specific ELISAs, as described previously (24).

Mice

SW$_{HEL}$ mice expressing a knock-in BCR against hen egg lysozyme (HEL) (15) were maintained on a C57BL/6J or C57BL/6-SJL.Ptprc$^{a/a}$ congenic background. Thy1.1 congenic mice (000406; B6.PL-*Thy1ª*/CyJ) (25) were crossed to OT2 TCR transgenic mice (B6.Cg-Tg(TcraTcrb425Cbn/J)) (26), and maintained on a C57BL/6 background. C57BL/6 and C57BL/6-SJL.Ptprc$^{a/a}$ congenic mice were purchased from Australian BioResources (Moss Vale, Australia). *Stk4*$^{Y88/Y88del}$ and *Stk4*$^{-/-}$ mice were produced by the Mouse Engineering Garvan/ABR (MEGA) Facility using CRISPR/Cas9 gene targeting in C57BL/6J mouse embryos following established molecular and animal husbandry techniques. A single guide RNA (sgRNA) was employed that targeted Cas9 to exon 4 of *Stk4,* adjacent to the Y88 codon (CCTCACGTAGTCAAG*TAT*TA<u>TGG</u>: Y88 codon italicized, protospacer-associated motif = PAM underlined). A solution consisting of sgRNA (15ng/µl), polyadenylated *S.pyogenes* Cas9 mRNA (30ng/µl) and a 150 base, single-stranded, deoxy-oligonucleotide homologous recombination substrate lacking the Y88 codon (54 bases 5' plus 96 bases 3', 10ng/µl) was prepared and microinjected into the nucleus and cytoplasm of C57BL/6J zygotes. Microinjected embryos were cultured overnight and those that underwent cleavage introduced into pseudo-pregnant foster mothers. Pups were screened by PCR across the target site and Sanger sequencing of PCR products used to detect mice carrying (1) a 2bp frame shift insertion or (2) specific removal of the Y88 codon which were then bred on a C57BL/6J background to establish the *Stk4*$^{-/-}$ and *Stk4*$^{Y88del/Y88del}$ lines, respectively. *Stk4*$^{Y88del/Y88del}$ and *Stk4*$^{-/-}$ mice were crossed to SW$_{HEL}$ mice on a C57BL/6-SJL.Ptprc$^{a/a}$ congenic background. For bone marrow chimeras, C57BL/6-SJL.Ptprc$^{a/a}$ (CD45.1$^+$) mice were irradiated in two doses, 6 hours apart, with 425 Rad (X-RADA 320 Biological Irradiator, PXI) and injected with 2 x 10^6 bone marrow cells (50:50 mixture of wild-type C57BL/6 CD45.1$^+$ bone marrow and either *Stk4*$^{Y88del/Y88del}$ or *Stk4*$^{+/+}$ CD45.2$^+$ marrow). They were allowed to reconstitute for 8-10 weeks before analysis or immunisation. All mice were bred and maintained in specific-pathogen free conditions at Australian BioResources (Moss Vale) and the Garvan Institute Biological Testing Facility. Animal experiments were approved by the Garvan Institute of Medical Research/St Vincent's Hospital Animal Ethics Committee.

Immunisations and adoptive cell transfer
SRBC immunisation

For SRBC immunisation, mice were given i.v. injection of 2×10^8 SRBCs (Alsevers) in 200μL. Splenocytes were harvested at d7 post immunisation and analysed by flow cytometry. To detect anti-SRBC antibodies in the serum, 2×10^6 SRBCs were plated in individual wells of a 96 well plate and SRBCs then incubated with serum dilutions from SRBC immunised mice. Serum from non-SRBC immunised mice was included as a negative control. Anti-SRBC antibodies were detected with anti-kappa biotin and SA-A647. Samples were acquired on a CytoPlate (Beckman Coulter).

HEL-SRBC immunisation

Purified hen egg lysozyme (HEL) was purchased from Sigma-Aldrich. Recombinant mutant HEL^{2X} and HEL^{3X} proteins with intermediate and low affinity for the HyHEL10 BCR were grown ns in yeast (*Pichia pastoris*) and purified from culture supernatants as described (27). For adoptive transfers, spleen cells from donor SW$_{HEL}$ mice containing 3×10^4 HEL-binding B cells were transferred i.v. into wild-type recipient mice together with 2×10^8 HEL^{2X}-SRBC or HEL^{3X}-SRBC, conjugated as previously describe (27).

HEL-OVA immunisation

OT2 T cells were enriched by negative depletion with biotinylated antibodies for anti-B220 clone RA3-6B2, anti-CD11b clone M1/70, anti-CD11c clone HL3, anti-CD8 clone, and *Stk4$^{+/+}$*, *Stk4$^{Y88del/Y88del}$* or *Stk4$^{-/-}$* SW$_{HEL}$ B cells were enriched by negative depletion with biotinylated antibodies for anti-CD11b, anti-CD11c, anti-CD4 clone GK1.5, anti-CD43 clone S7 (all from BD Bisociences) and MACs anti-biotin magnetic beads (Miltenyi). Purity of CD4$^+$ V$_\alpha$2$^+$ OT2 T cells was typically 70-80% and B220$^+$ HEL-binding SW$_{HEL}$ B cells >99% as determined by FACs analysis. 2.5×10^5 CD4$^+$Vα2$^+$ OT2 T cells and B220$^+$ HEL-binding SW$_{HEL}$ B cells were adoptively transferred into age and sex matched 6-9 week old recipient mice. Recipient mice were immunised the next day by subcutaneous injection with 20μg HEL-OVA in Sigma Adjuvant System (SAS) in the lower flank and base of tail. For memory responses, mice that had been immunised were rested for at least 28 days and then re-challenged with 40μg HEL-OVA in SAS injected subcutaneously in the lower flank and base of tail. HEL was conjugated to OVA$_{323-339}$ peptide (CGGISQAVHAAHAEINEAGR) (Mimotopes/Genscript) using the SMPH cross-linking agent Succinimidyl-6-([ß-maleimidopropionamido] hexanoate) (Thermo Fisher Scientific).

BrdU incorporation

1mg bromodeoxyuridine (BrdU) (Sigma) was injected i.v. into recipient mice, and harvested 1hr post injection. Splenocytes were surface stained, then samples fixed, permeabilised and stained with anti-BrdU-FITC using the BrdU flow kit (BD Biosciences) as per the manufacturers protocol.

FACS analysis of mouse cells

Spleen and inguinal lymph nodes were harvested, dissected free of fat and fascia, and lymph nodes teased apart with microforceps and mashed through a 70μm filter. Bone marrow cells were harvested from tibia and femur by centrifugation and peritoneal cavity cells were harvested by peritoneal lavage. Blood was collected by cardiac puncture for FACS analysis into ~50uL heparin solution, or allowed to clot at room temperature and collected serum stored at -20°C for future ELISAs. Spleen, bone marrow and blood samples were RBC lysed. Single cell suspensions were then washed and Fc receptors blocked with unlabeled anti-CD16/32 clone 2.4G2 before staining. To detect HEL-binding B cells, cells were stained with saturating levels of HEL at 200 ng/ml, followed by HyHEL9 Alexa Fluor 647. For detection of HEL-binding IgG1$^+$ B cells, anti-IgG1 staining was performed first and followed by blocking with 5% mouse serum before subsequent staining for HEL-binding with HyHEL9, a mouse IgG1 monoclonal antibody. Antibodies used for surface staining are shown in Table 1. For intracellular staining, cells were fixed with Fixation/Permeabilization buffer and antibodies stained in Permeabilization buffer (eBioscience). Antibodies used for intracellular staining were: anti-FOXO1 (C29H4, CST) detected with anti-rabbit FITC (Southern Biotech) and anti-active caspase-3 (C92-605, BD Biosciences). Cells were filtered using 35 μm filter round-bottom FACS tubes (BD Biosciences) immediately before data acquisition on either an LSR II SORP or Fortessa (BD) and data analysed using FlowJo software (Tree Star, Inc.).

Table 2 – Mouse antibodies

TARGET	CLONE	CONJUGATION	SOURCE
B220	RA3-6B2	BV650	Biolegend
		biotin, FITC, PE, Pacific Blue, BV786	BD Biosciences
BrdU	-	FITC	BD Biosciences
Caspase-3 (active)	C92-605	PE	BD Biosciences
CD11b	M1/70	biotin	BD Biosciences
CD11c	HL3	biotin	BD Biosciences
CD16/32	2.4G2	purified	BioXCell
CD138	281-2	PE, BV650	BD Biosciences
CD19	ID3	APC, BV510	BD Biosciences
CD21/CD35	7E9	Pacific Blue	Biolegend
CD23	B3B4	PE-Cy7	eBioscience
CD24	M1169	PE	BD Biosciences
CD3	eBio500A2	FITC, biotin	eBioscience
CD38	90	BV510, FITC, PerCPCy5.5	BD Biosciences
CD4	GK1.5	biotin	BD Biosciences
	RM4-5	Pacific Blue	BD Biosciences
		BV785	Biolegend
CD43	S7	biotin, BV421	BD Biosciences
CD44	Ly-24	FITC	BD Biosciences
		APC	BD Biosciences
CD45.1	A20	PerCPCY5.5	Biolegend
		PE	BD Biosciences
		FITC, PE-Cy7	eBioscience
CD45.2	104	PE-Cy7	Biolegend
		BUV395	BD Biosciences
CD5	53-7a	PE	BD Biosciences
CD62L	MEL-14	FITC, PE	BD Biosciences
CD69	H1.2F3	FITC, PE, BV421	BD Biosciences
CD8	53-6.7	biotin	Biolegend
		Pacific Blue	BD Biosciences
CD86	GL-1	PE	BD Biosciences
		BV650	Biolegend
CD93	AA4.1	PE	eBioscience
		PerCPCy5.5	Biolegend
CXCR4	2B11	BV421	BD Biosciences
Fas	Jo2	PE-Cy7, BV510, biotin	BD Biosciences
FITC	-	Alexa Fluor 488	Jackson ImmunoResearch
FOXO1	C29H4	purified	Cell Signaling Technologies
HyHEL9	-	A647	Conjugated in house
HEL	-	Polyclonal rabbit	Rockland
IgA	C10-3	Purified	BD Biosciences

IgD	11-26c.2a	FITC	BD Biosciences
		Alexa Fluor 647, APC-Cy7	Biolegend
IgE	R35-72	Purified	BD Biosciences
IgG Fcγ fragment	-	Purified	Jackson ImmunoResearch
IgG1	A85-1	FITC, PE, biotin	BD Biosciences
IgM	II-41	Purified, PE-Cy7	eBioscience
IgMb	A56-78	FITC	Biolegend
Kappa	187.1	biotin	BD Biosciences
MAdCam-1	MECA367	biotin	Biolegend
Rabbit	Goat polyclonal	FITC	Southern Biotech
Streptavidin	-	Alexa Fluor 647, Alexa Fluor 555	Invitrogen
		PE-Cy7	eBioscience
		PE, BV421, BV786, BUV395	BD Biosciences
Vα2	B20.1	FITC, APC	eBioscience

Mouse SHM analysis

SW$_{HEL}$ GC B Cells (B220$^+$ CD45.1$^+$ Fas$^+$ CD38$^-$ IgD$^-$) were sorted from recipient mice using FACS Aria III (BD Biosciences) 13d after transfer and immunisation with HEL^{3X}-SRBC and deposited as single cells in 96 well plates. The SW$_{HEL}$ heavy chain variable region was amplified from genomic DNA by nested PCR and products were sequenced and analysed.

Mouse ELISAs

Isotype specific polyclonal antibody levels from unimmunised mice and anti-HEL antibody levels in sera from immunised mice were analysed by ELISA. In brief, 384 well flat bottom plates (Nunc) were coated overnight at 4°C with specific isotype for unimmunised mice or HEL, HEL^{2x} or HEL^{3x} at 10μg/mL for HEL$^{2x/3x}$ immunized mice. The wells were then blocked with 1% BSA/PBS and serial dilutions of sera added together with appropriate standards. Biotinylated anti-kappa for unimmunised mice or IgG1 from HEL$^{2X/3X}$ immunised mice in 0.1% BSA/1% skim milk powder/PBS was used to detect bound antibody. SA-alkaline phosphatase in 0.1% BSA was then added and visualized with the substrate *p*-nitrophenyl phosphate (1mg/mL) in NPP buffer. Absorbance at 405nm was read and the concentration of isotype specific polyclonal antibodies or anti-HEL antibodies calculated from the standard curve.

Mouse epifluorescence microscopy

Spleens were snap frozen in cryomolds with OCT (Tissue Tek). 7μm sections were cut using a CM3050S cryostat (Leica), transferred to PolySine glass slides and air-dried. Cut sections were fixed in ice-cold acetone, dried and blocked with 30% horse serum (Invitrogen), 3% BSA in PBS. Sections were subsequently stained with antibodies described and visualized on a Leica DM5500 microscope. Images were compiled and brightness and contrast adjusted in Adobe Photoshop.

Mouse in vitro B cell stimulation

Lymph node cells were cultured overnight at 37°C with or without HEL (200ng/mL) in B cell medium and activation surface marker expression analysed 18 hours later by FACS analysis.

Retroviral transduction

Anti-CD40 mAb (BioXCell) and IL-4 (R & D systems) cultured SW$_{HEL}$ spleens were retrovirally transduced with genes encoding FOXO1 or empty cassette, transferred into recipient mice and immunised with HEL^{3X}-SRBC. Donor response was analysed by flow cytometry as described above.

Western blot

Red blood cell lysed mouse spleenocytes were washed in chilled PBS then cell lysed with NP40 buffer with protease inhibitors, reduced with reducing buffer for 10 minutes at 70°C and western blot for STK4 (CST, 14946) and GAPDH (Santa Cruz, SC-32233) protein levels performed.
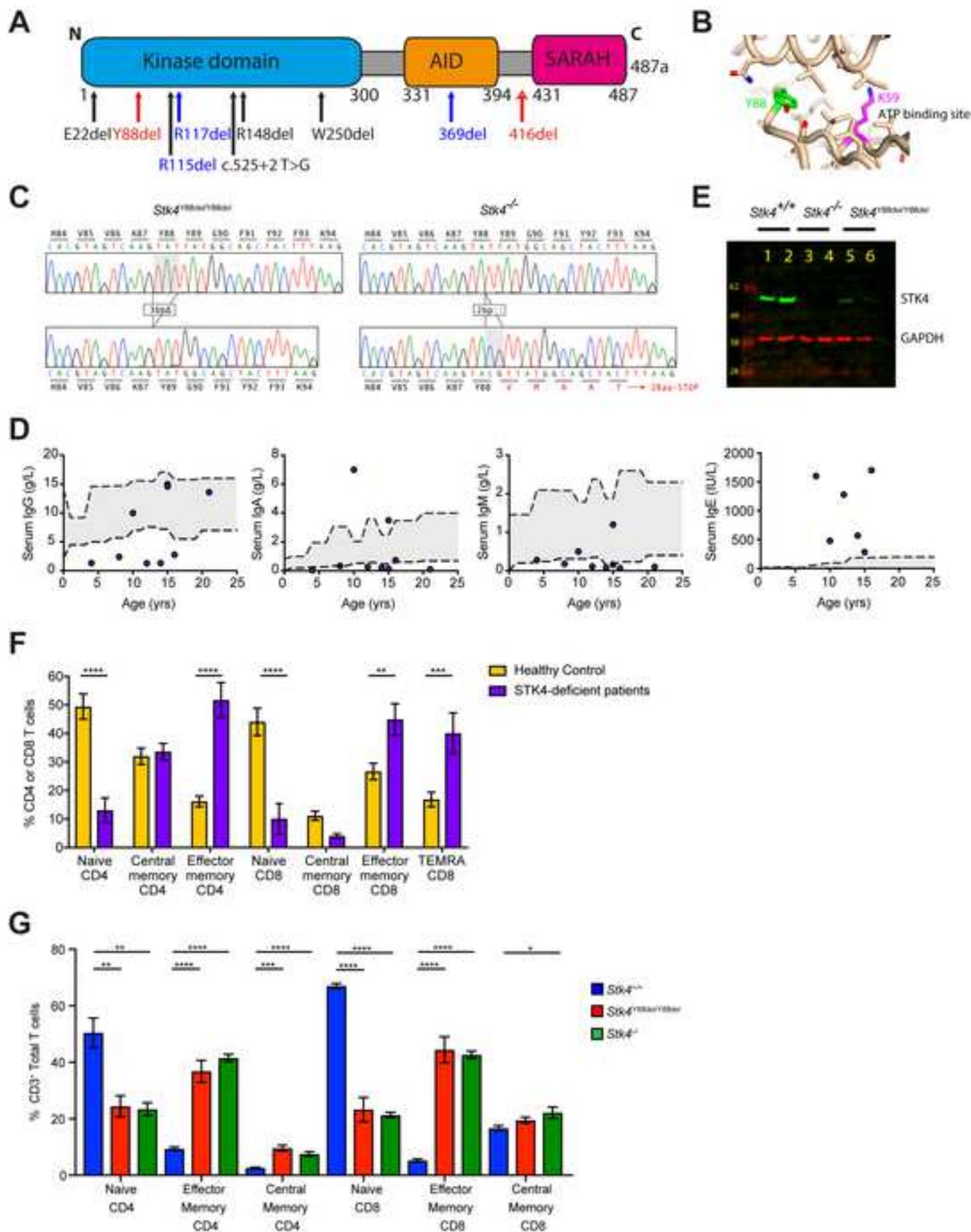
Statistical Analysis

Data was analysed with Prism software (GraphPad). For comparison between two normally distributed groups a one-tailed unpaired Student's t-test with Welch's correction was used, and for more than two groups we used one-way ANOVA with Tukey's correction for multiple comparisons. Non-parametric data was analysed by Mann-Whitney U test. Differences between multiple paired measurements were analysed by the Wilcoxon signed-rank test. * $p < 0.05$, ** $p < 0.01$, *** $p < 0.001$ and **** $p < 0.0001$.
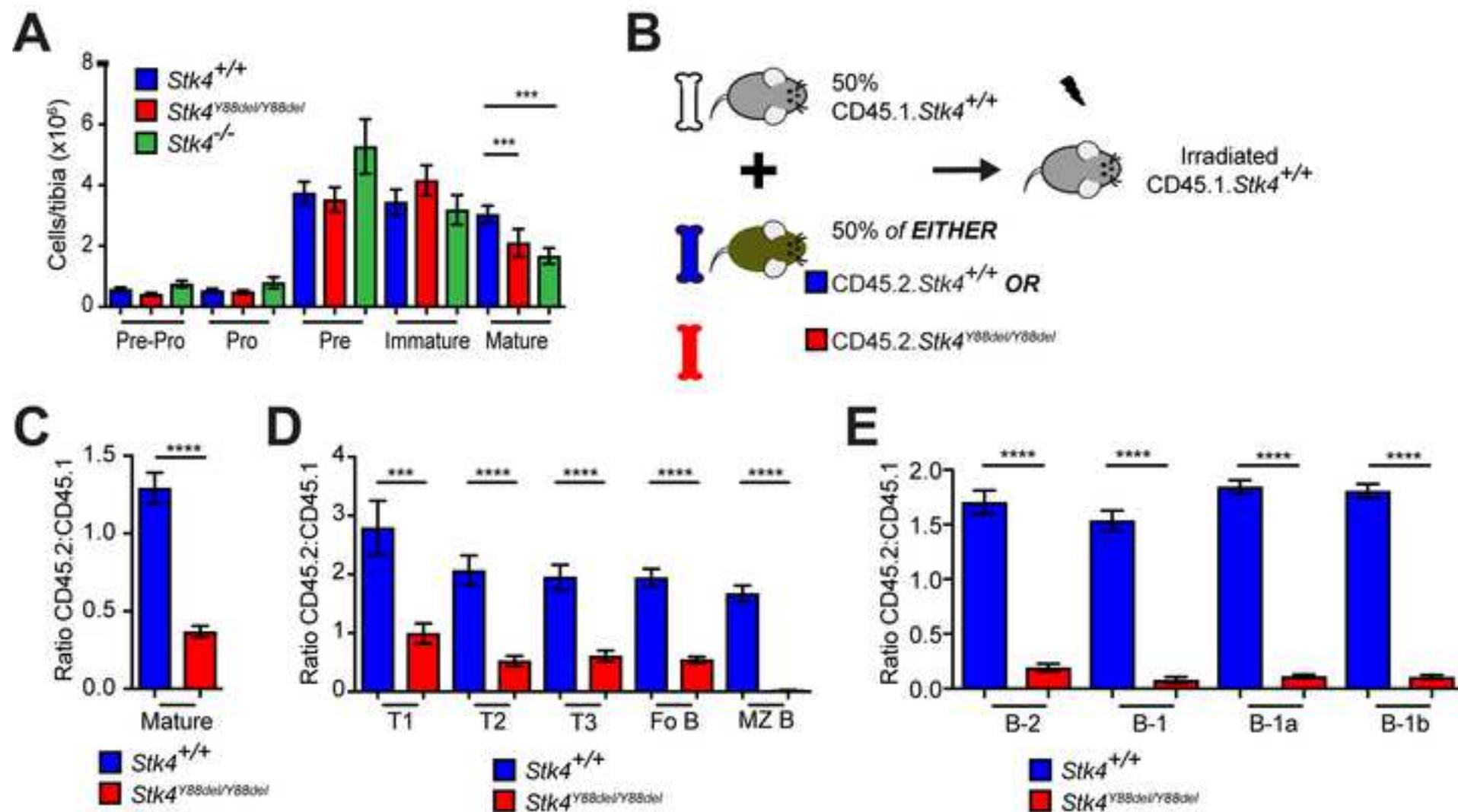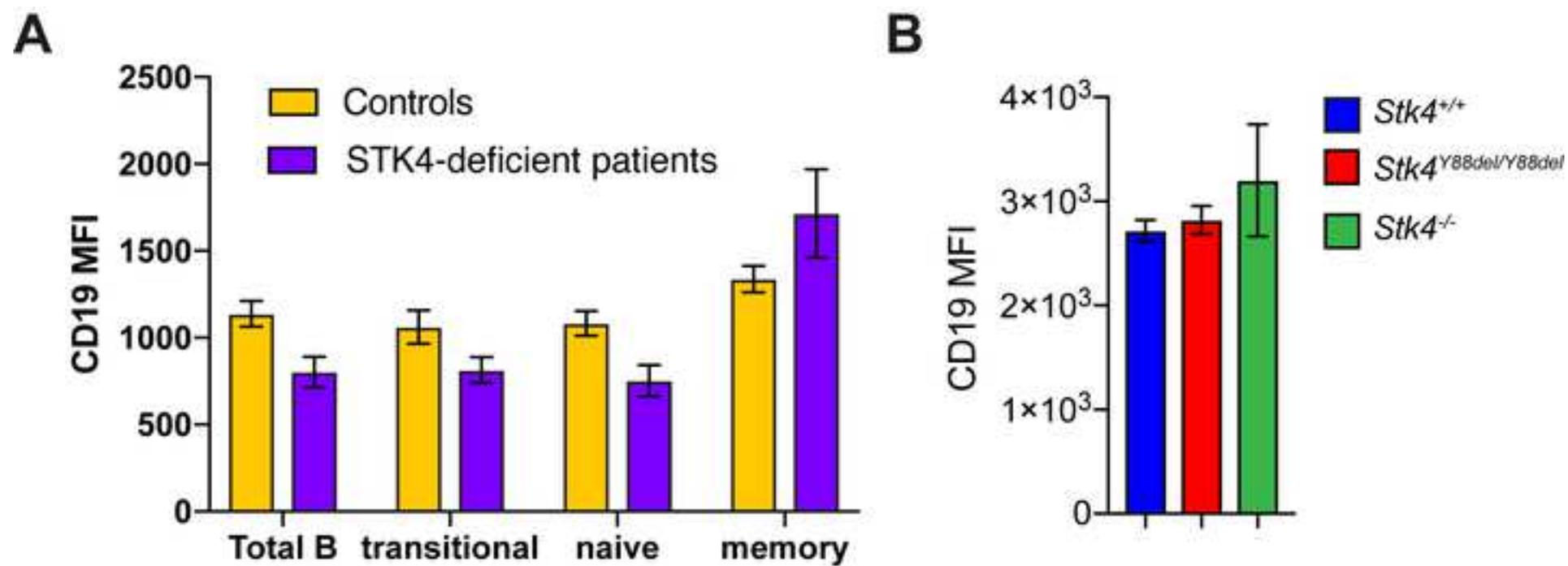
Extended References

1.   Abdollahpour H, Appaswamy G, Kotlarz D, Diestelhorst J, Beier R, Schäffer AA, et al. The phenotype of human STK4 deficiency. *Blood*. 2012;119(15):3450-7.

2.   Nehme NT, Schmid JP, Debeurme F, André-Schmutz I, Lim A, Nitschke P, et al. MST1 mutations in autosomal recessive primary immunodeficiency characterized by defective naive T-cell survival. *Blood*. 2012;119(15):3458-68.

3.   Halacli SO, Ayvaz DC, Sun-Tan C, Erman B, Uz E, Yilmaz DY, et al. STK4 (MST1) deficiency in two siblings with autoimmune cytopenias: A novel mutation. *Clinical Immunology*. 2015;161(2):316-23.

4.   Crequer A, Picard C, Patin E, D'Amico A, Abhyankar A, Munzer M, et al. Inherited MST1 Deficiency Underlies Susceptibility to EV-HPV Infections. *PLOS ONE*. 2012;7(8):e44010.

5.   Dang TS, Willet JDP, Griffin HR, Morgan NV, O'Boyle G, Arkwright PD, et al. Defective Leukocyte Adhesion and Chemotaxis Contributes to Combined Immunodeficiency in Humans with Autosomal Recessive MST1 Deficiency. *Journal of Clinical Immunology*. 2016;36(2):117-22.
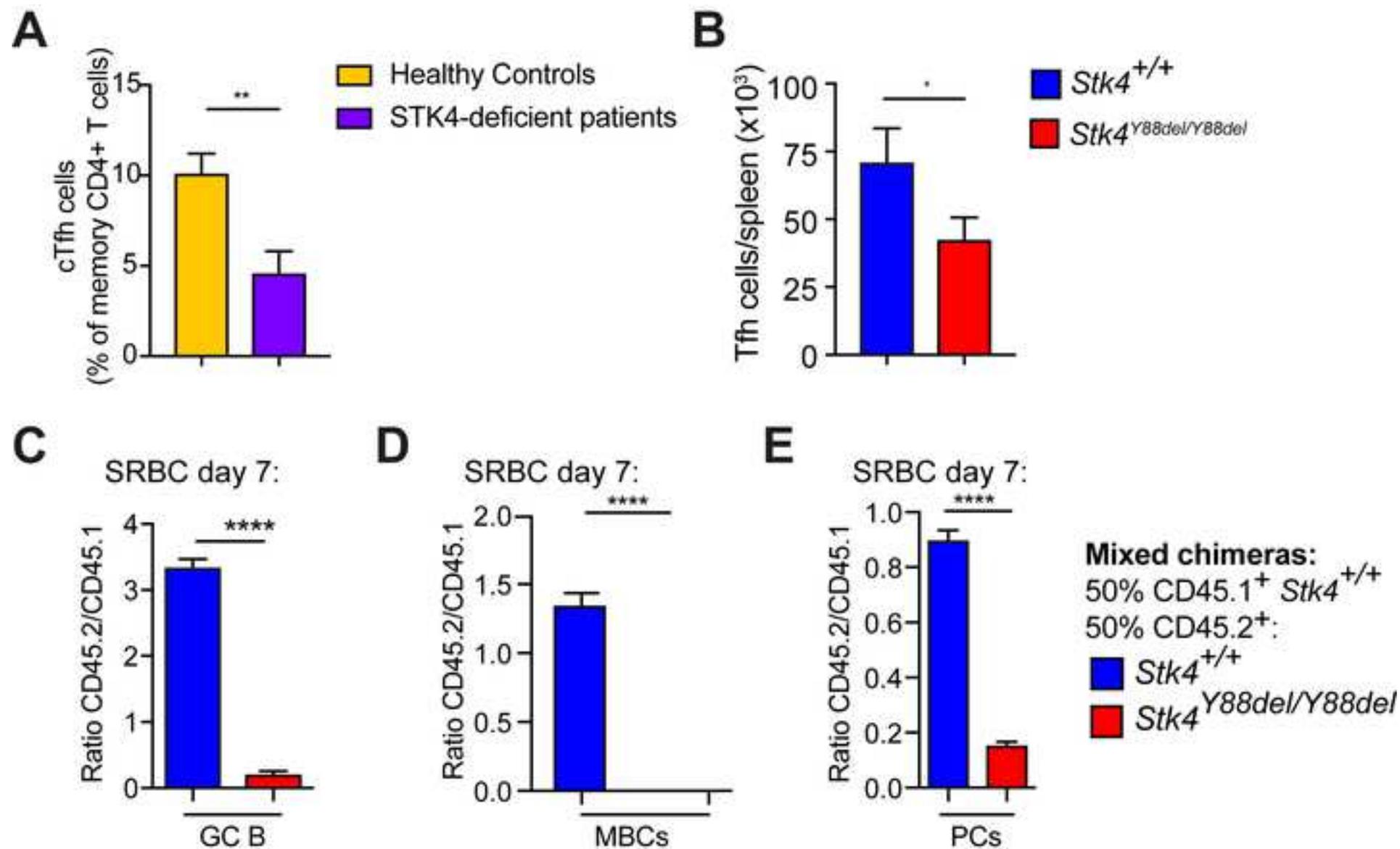
6.   Schipp C, Fischer U, Schlütermann D, Hönscheid A, Nabhani S, Höll J, et al. EBV Negative Lymphoma and Autoimmune Lymphoproliferative Syndrome Like Phenotype Extend the Clinical Spectrum of Primary Immunodeficiency Caused by STK4 Deficiency. *Frontiers in Immunology*. 2018;9

7.   Kurz AR, Pruenster M, Rohwedder I, Ramadass M, Schafer K, Harrison U, et al. MST1-dependent vesicle trafficking regulates neutrophil transmigration through the vascular basement membrane. *J Clin Invest*. 2016;126(11):4125-39.

8.   Li C, Bi Y, Li Y, Yang H, Yu Q, Wang J, et al. Dendritic cell MST1 inhibits Th17 differentiation. *Nat Commun*. 2017;8:14275.

9.   Katagiri K, Katakai T, Ebisuno Y, Ueda Y, Okada T, Kinashi T. Mst1 controls lymphocyte trafficking and interstitial motility within lymph nodes. *EMBO J*. 2009;28(9):1319-31.

10.   Dong Y, Du X, Ye J, Han M, Xu T, Zhuang Y, et al. A cell-intrinsic role for Mst1 in regulating thymocyte egress. *J Immunol*. 2009;183(6):3865-72.

11.   Li W, Xiao J, Zhou X, Xu M, Hu C, Xu X, et al. STK4 regulates TLR pathways and protects against chronic inflammation-related hepatocellular carcinoma. *J Clin Invest*. 2015;125(11):4239-54.

12.   Bai X, Huang L, Niu L, Zhang Y, Wang J, Sun X, et al. Mst1 positively regulates B-cell receptor signaling via CD19 transcriptional levels. *Blood Adv*. 2016;1(3):219-30.

13.   Zhou D, Medoff BD, Chen L, Li L, Zhang XF, Praskova M, et al. The Nore1B/Mst1 complex restrains antigen receptor-induced proliferation of naive T cells. *Proc Natl Acad Sci U S A*. 2008;105(51):20321-6.

14.   Alsufyani F, Mattoo H, Zhou D, Cariappa A, Van Buren D, Hock H, et al. The Mst1 Kinase Is Required for Follicular B Cell Homing and B-1 B Cell Development. *Front Immunol*. 2018;9(2393)

15.   Phan TG, Amesbury M, Gardam S, Crosbie J, Hasbold J, Hodgkin PD, et al. B cell receptor-independent stimuli trigger immunoglobulin (Ig) class switch recombination and production of IgG autoantibodies by anergic self-reactive B cells. *J Exp Med*. 2003;197(7):845-60.

16.   Phan TG, Paus D, Chan TD, Turner ML, Nutt SL, Basten A, et al. High affinity germinal center B cells are actively selected into the plasma cell compartment. *J Exp Med*. 2006;203(11):2419-24.

17.   Harvey KF, Pfleger CM, Hariharan IK. The Drosophila Mst ortholog, hippo, restricts growth and cell proliferation and promotes apoptosis. *Cell*. 2003;114(4):457-67.

18.   Wilkinson DS, Jariwala JS, Anderson E, Mitra K, Meisenhelder J, Chang JT, et al. Phosphorylation of LC3 by the Hippo kinases STK3/STK4 is essential for autophagy. *Mol Cell*. 2015;57(1):55-68.
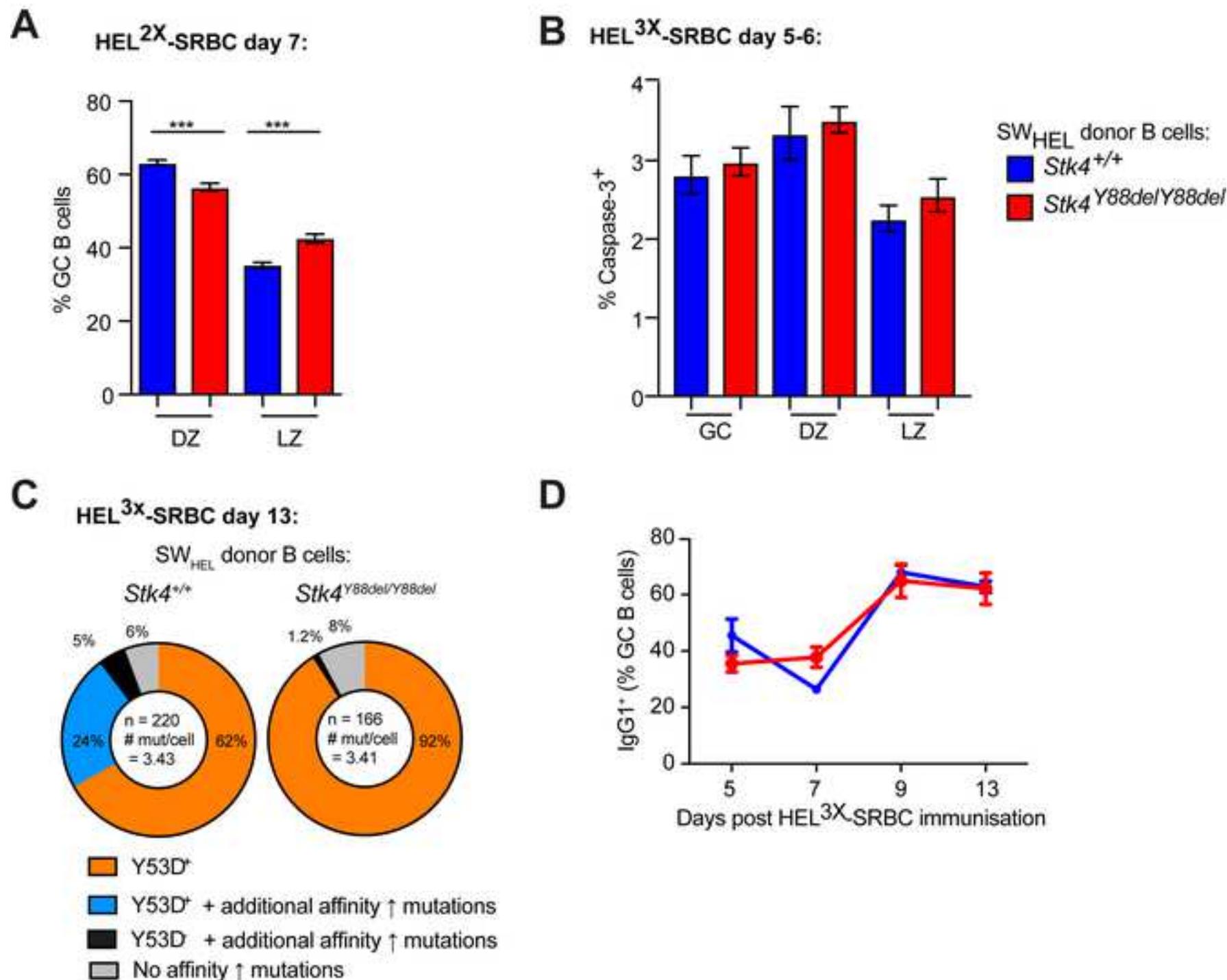
19.   Lehtinen MK, Yuan Z, Boag PR, Yang Y, Villen J, Becker EB, et al. A conserved MST-FOXO signaling pathway mediates oxidative-stress responses and extends life span. *Cell*. 2006;125(5):987-1001.

20.   Inoue T, Shinnakasu R, Ise W, Kawai C, Egawa T, Kurosaki T. The transcription factor Foxo1 controls germinal center B cell proliferation in response to T cell help. *J Exp Med*. 2017;214(4):1181-98.

21.   Dominguez-Sola D, Kung J, Holmes AB, Wells VA, Mo T, Basso K, et al. The FOXO1 Transcription Factor Instructs the Germinal Center Dark Zone Program. *Immunity*. 2015;43(6):1064-74.

22.   Sander S, Chu VT, Yasuda T, Franklin A, Graf R, Calado DP, et al. PI3 Kinase and FOXO1 Transcription Factor Activity Differentially Control B Cells in the Germinal Center Light and Dark Zones. *Immunity*. 2015;43(6):1075-86.

23.   Avery DT, Kane A, Nguyen T, Lau A, Nguyen A, Lenthall H, et al. Germline-activating mutations in PIK3CD compromise B cell development and function. *J Exp Med*. 2018;215(8):2073-95.

24.   Avery DT, Deenick EK, Ma CS, Suryani S, Simpson N, Chew GY, et al. B cell-intrinsic signaling through IL-21 receptor and STAT3 is required for establishing long-lived antibody responses in humans. *J Exp Med*. 2010;207(1):155-71.

25.   Snell G, Cherry M. Loci determining cell surface antigens. In: Emmelot P, Bentvelsen P, editors. RNA Viruses and Host Genome in Oncogenesis. Amsterdam, North Holland1972.

26.   Barnden MJ, Allison J, Heath WR, Carbone FR. Defective TCR expression in transgenic mice constructed using cDNA-based alpha- and beta-chain genes under the control of heterologous regulatory elements. *Immunol Cell Biol*. 1998;76(1):34-40.

27.   Paus D, Phan TG, Chan TD, Gardam S, Basten A, Brink R. Antigen recognition strength regulates the choice between extrafollicular plasma cell and germinal center B cell differentiation. *J Exp Med*. 2006;203(4):1081-91.
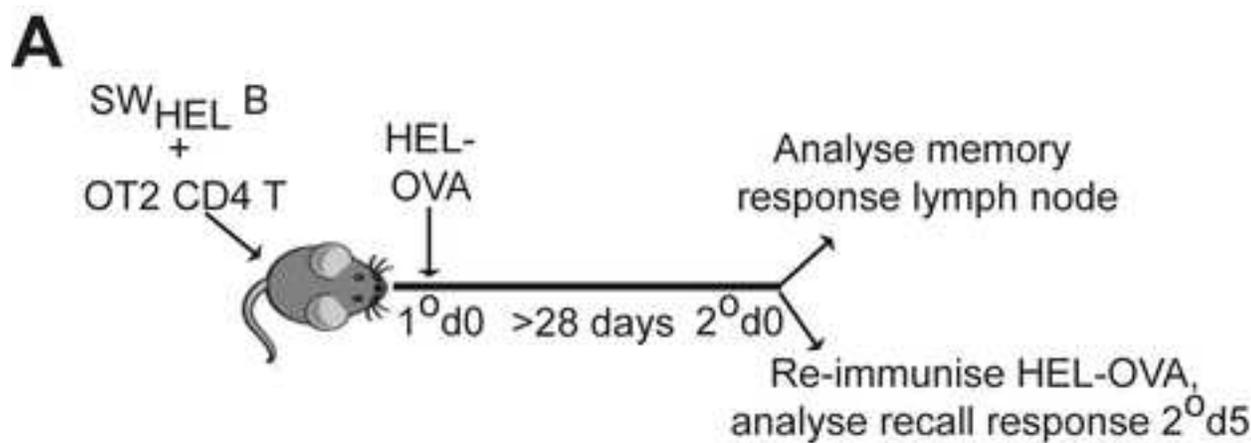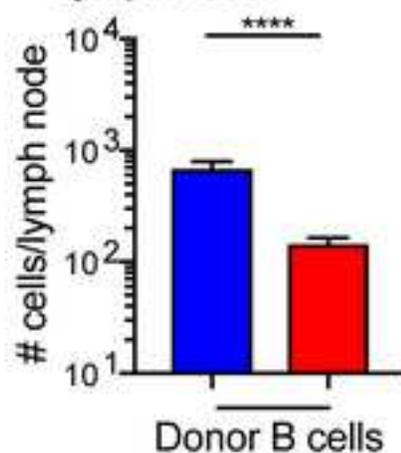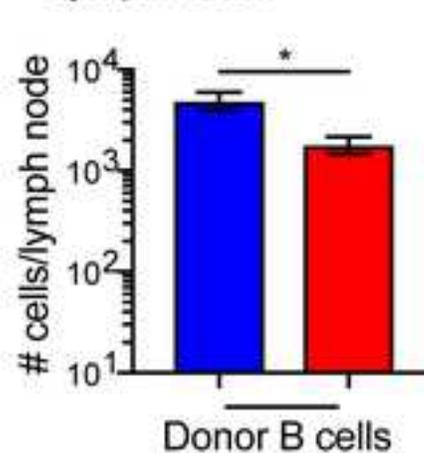
A

SW$_{HEL}$ B
+
OT2 CD4 T

HEL-OVA

Analyse memory response lymph node

1^{O}d0   >28 days 2^{O}d0

Re-immunise HEL-OVA, analyse recall response 2^{O}d5

B HEL-OVA memory Lymph node:

cells/lymph node

****

Donor B cells

C HEL-OVA 2^O day 5 Lymph node:

cells/lymph node

*

Donor B cells

SW$_{HEL}$ donor B cells:

$Stk4^{+/+}$ $Stk4^{Y88del/Y88del}$

D

Memory B cell culture 7 days, CD40L/IL-21

hu Ig secretion (ng/ml)

● Control
● STK4 patient

IgM   IgG   IgA

A SRBC day 7:

Stk4$^{+/+}$
Stk4$^{Y88del/Y88del}$
Stk4$^{-/-}$

FOXO1 MFI

GC B   Total B

B HEL^{3X}-SRBC day 7:

Donor % lymphocytes

Transduction:
○ Empty vector
● FOXO1

WT   Y88   WT   Y88

SW$_{HEL}$ donor